Ultra-wideband communications using hybrid matched filter correlation receivers

Tufvesson, Fredrik; Gezici, Sinan; Molisch, Andreas

Published in:
IEEE Transactions on Wireless Communications

DOI:
10.1109/TWC.2006.04767

2006

Ultra-Wideband Communications using Hybrid Matched Filter Correlation Receivers

Fredrik Tufvesson, *Member, IEEE*, Sinan Gezici, *Member, IEEE*, and Andreas F. Molisch, *Fellow, IEEE*

***Abstract*— Transmitted-reference (TR) schemes for time-hopping impulse radio (TH-IR) ultra-wideband (UWB) communications allow the use of simple receiver structures that are able to combine energy from different multipath components without channel estimation. A conventional TR receiver consists of a simple delay-and-multiply operation combined with an integrator. On the downside, it shows a performance loss due to non-linear operations on noise terms (generation of noise-noise cross-terms) when forming the decision variable. This paper describes a hybrid receiver structure for UWB communications that reduces these noise-noise cross-terms by first performing a "matched filtering" operation matched to the time-hopping sequence of pulses. The receiver retains most of the simplicity of the conventional TR receiver, but requires an analog correlator for the time-hopping sequence of pulses. The performance the proposed receiver is analyzed in both AWGN and multipath channels. For the AWGN case, the exact expression for the bit error probability is obtained, which takes into account the non-Gaussian nature of the noise-noise cross-terms arising in the correlators. For the multipath case, both inter-frame interference and multipath interference from the reference pulse to the data pulse are considered, and approximate closed-form expressions are derived based on the assumption of a large integration interval. Also approximate criteria for optimal integration interval are obtained for the best receiver performance. Simulation studies are presented to analyze the performance of the proposed receiver structure and to confirm the theoretical analysis.**

***Index Terms*— Ultra-wideband (UWB), impulse radio (IR), transmitted-reference (TR), multipath channels, inter-frame interference (IFI), receivers.**

I. Introduction

ULTRA-WIDEBAND (UWB) communications systems are defined as systems that have either a relative bandwidth of more than 20%, or an absolute bandwidth of more than 500 MHz. The report and order of the Federal Communications Commission (FCC) in the U.S. [1] allowed unlicensed operation of UWB communications, which has greatly increased the interest in these systems. UWB communications have traditionally been associated with impulse radio (IR) [2], [3], which is well suited for low-data-rate communications, and most of the academic work on UWB has concentrated on IR for the last 10 years. The recent formation of the IEEE 802.15.4a group, which will establish a standard for probably UWB-based low-data-rate communications, has also created considerable commercial interest for such systems [4].

An IR system transmits information by modulating the amplitude or position (delay) of very short (on the order of 100 ps to 2 ns) pulses. In order to permit several users to communicate simultaneously, a bit is not represented by a single pulse, but rather by a *sequence* of pulses, where the position of each pulse is determined by a pseudo-random sequence assigned to each user. The symbol duration is divided into N_f intervals called "frames", each of which contains one pulse. The pseudo-random sequence that determines the locations of the pulses within the frames is called a time-hopping (TH) code [5], which reduces the probability of "catastrophic collisions" between two simultaneously transmitting users.

Due to the wide bandwidth, IR receivers can resolve many multipath components in the received signal, and have to add them up in order to "collect" all the received energy [6]. The optimum scheme to achieve this is a Rake receiver, combined with a receive filter matched to the received pulse [3]. This scheme provides a high degree of delay diversity; as a matter of fact, the fine delay resolution has long been considered a major advantage of UWB systems. However, the Rake requires a fairly complicated receiver structure, with one despreader (correlator, Rake finger) for each multipath component to be received. Therefore, often only the strongest, or a few of the strongest, paths are used to form the decision variable [7], [8]. This, of course, means that the receiver does not collect energy from all the multipath components and therefore there is a performance loss compared to the ideal case. Furthermore, a Rake receiver needs to estimate the channel impulse response in order to obtain the correct Rake weights [9], [10].

All these issues have led to an increased interest in so-called "transmitted reference" (TR) schemes [8], [11]-[14]. Reference [11] first suggested the scheme for UWB, and also presented some experimental results in a companion paper [15]. In a TR scheme, channel estimation and despreading is done in one simple step. For that purpose, two pulses are transmitted in each frame. The first pulse is not modulated and is called the reference pulse. The second pulse, which is modulated, is separated by a time delay T_d from the first pulse, and is called the data pulse. The receiver uses pulse-pair correlators to recover the data, which means that the signal is multiplied by a delayed version of itself. Each multipath component results in a peak at the output of the multiplier

Manuscript received November 23, 2004; revised August 31, 2005, November 20, 2005, and May 4, 2006; accepted June 21, 2006. The associate editor coordinating the review of this paper and approving it for publication was Z. Tian. Part of this work was presented at IEEE VTC spring 2004 and IEEE Globecom 2004. Part of this work was financially supported by an INGVAR grant of the Swedish Strategic Research Foundation.

F. Tufvesson is with the Department of Electroscience, Lund University, Box 118, SE-221 00 Lund, Sweden (email: fredrik.tufvesson@es.lth.se).

S. Gezici is with Mitsubishi Electric Research Labs, 201 Broadway, Cambridge, MA 02139 (email: gezici@ieee.org).

A. F. Molisch is with Mitsubishi Electric Research Labs, 201 Broadway, Cambridge, MA 02139, and also at the Department of Electroscience, Lund University, Box 118, SE-221 00 Lund, Sweden (email: Andreas.Molisch@ieee.org).

Digital Object Identifier 10.1109/TWC.2006.04767.

with the same phase (which is determined by the value of the data symbol), and therefore these contributions from multipath components can be summed by an integrator. The integrator output is detected in a conventional way to make a decision on the transmitted data symbols. The scheme thus shows a fundamental similarity to differential detection.

The advantage of TR schemes is the fact that they allow for very simple receiver structures. Their main drawback stems from a reduced signal-to-noise ratio (SNR). This reduction is partly due to "wasting" energy on the reference pulses that are not carrying any information. More importantly, the differential detection gives rise to excess noise related to the multiplication of noise contributions in the received reference pulses with the noise contributions in the received data pulses. Those cross-terms are especially troublesome in a UWB receiver: the input to the multiplication operator has a very low SNR, because those are the signals *before* the despreading operation. This results in large noise-noise terms that are integrated over a certain time interval. References [8] and [12] suggested averaging the reference pulses over several pulse durations, in order to reduce the noise in the reference pulses, and thus also the cross-terms. For the same purpose, [16] considered a feedback loop TR receiver, which reduces the noise in the reference pulses by using the previous information symbols. The important paper of [8] also gives a detailed derivation of the error probability for both the conventional TR receiver and the receiver that uses averaged reference pulses.

Another important issue to consider in TR systems is the interference between the pulses. There can be both inter-frame interference (IFI) and interference between the reference and the data pulses. Almost all of the previous studies ignore the effects of those interference terms [12], [14], [17], [18] [1].

In this paper, we introduce a new differential receiver structure that has a performance similar to that of [8]. The proposed receiver requires an analog correlator for the TH sequence of pulses, but is otherwise easier to implement. We also present a performance analysis that is more general than the previous results. Specifically, the new contributions of our paper include:

- we present a receiver structure that requires only *symbol*-rate sampling, not *frame*-rate sampling, while greatly reducing noise-noise contributions
- we analyze the effect of the non-Gaussian nature of the noise-noise cross-terms
- we analyze a system that uses BPSK as modulation format, and polarity randomization of the pulse sequence. BPSK gives a better receiver SNR [21], and the polarity randomization results in a transmit spectrum that better exploits the FCC mask [22]
- we analyze the impact of IFI, and the interference from the reference pulse to the data pulse. This is vital for systems with moderate to high data rates
- we simulate the performance of a TR scheme in the standardized IEEE 802.15.3a channel models [23].

[1]Parallel to our work in [19], [20] investigated the impact of IFI, and calculated its moments. However, it assumes no thermal noise in the system in order to facilitate the calculations.

The paper is organized the following way: Section II describes our new hybrid receiver structure, and discusses the implementation issues of the scheme. Section III derives the exact distribution of the noise in the system and obtains BEP expressions in AWGN channels. Section IV provides the BEP expressions for delay-dispersive channels, and the rules for optimal integration interval. Next, we present simulation results that confirm our theoretical analysis, and analyze the performance in the standardized IEEE channel models. A summary and conclusions wrap up the paper.

II. Transceiver Structure

A. Transmit Signal

The transmit signal from an IR TR system consist of a reference signal and a data signal. The transmitted signal is given by

$$s_{TX}(t) = \sqrt{\frac{E_s}{2N_f}} \sum_{j=-\infty}^{\infty} d_j [w_{tx}(t - jT_f - c_j T_c) + b_{\lfloor j/N_f \rfloor} w_{tx}(t - jT_f - c_j T_c - T_d)], \quad (1)$$

where $b_{\lfloor j/N_f \rfloor} \in \{-1, +1\}$ is the binary information symbol with N_f denoting the number of frames per symbol, T_c is the chip duration, T_f is the frame duration, and T_d is the delay between the reference pulse and the data pulse. We assume that $T_d = \Delta T_c$ where Δ is a positive integer. The c_j denote a (pseudo-)random integer sequence with values between 0 and $N_c - 1$, which determines the TH sequence; N_c is the number of chips per frame. The d_j denote a pseudo-random sequence of $+1$ and -1 that ensures a zero-mean output and is also helpful in shaping the transmit spectrum [22] according to the FCC rules [1]. We assume that the support of $w_{tx}(t)$, the unit-energy transmit waveform, extends only over one chip duration. E_s denotes the energy per transmitted symbol, and the symbol duration, T_s is given by $N_f T_f$. Note from (1) that there are one reference and one data pulse related to each frame, and the data pulse in one frame can overlap with the reference pulse in the next frame if there is no constraint on the TH codes. But conventionally, the TH codes are selected so as to contain both the data and the reference pulses in the related frame. But there can still occur IFI due to multipath propagation.

B. Conventional TR Receiver

Let $r(t)$ denote the received signal. The first step at the receiver is to pass $r(t)$ through a receive filter. As recommended by [8], this filter should be wide enough not to introduce any signal distortions, and just limit the available noise. The filtered receive signal $\widehat{r}(t)$ is multiplied with a delayed version of itself, and integrated over a finite interval T_{int}, determined by the excess delay and signal duration to achieve maximum SNR. The output of the integrator at time t_k is thus

$$\xi(t_k) = \int_{t_k - T_{int}}^{t_k} \widehat{r}(t)\widehat{r}(t - T_d)dt. \quad (2)$$

In [8], it is assumed that sampling occurs during each frame; the sampled (and A/D converted) ξ_k are then further processed to yield estimates of the received bits.

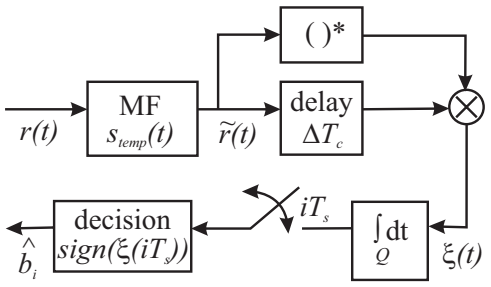

Fig. 1. Building blocks for the basic hybrid receiver. Note that the sampling circuit performs symbol rate sampling.

C. Hybrid Receiver Principle

As mentioned above, a main performance degradation of the TR receiver is due to the noise-noise cross-terms created by the multiplication process in a conventional TR receiver. As the input SNR of a spread spectrum UWB receiver is low, the noise-noise cross-terms are non-negligible - in contrast to conventional differential detection [21]. The key idea of our new receiver is to perform a despreading $before$ the multiplication operation. Thus, the SNR of the inputs to the multiplier is higher, and the relative impact of the noise-noise cross-terms is lower.

Fig. 1 shows a block diagram of the receiver. The receiver contains a filter matched to the reference signal. This filter results in a peak from the reference signal and a delayed peak from the data signal for each multipath component of the channel. The phase of these peaks are random, they depend on the channel. It is critical that this filter is matched to the whole *pulse sequence* representing one symbol, and not just the basis pulse within a frame. Subsequent processing is similar to the conventional TR receiver: the output of the filter matched to the reference signal is delayed by T_d and multiplied with itself. This product has also a peak for each multipath component, but the phases are now aligned and determined only by the data symbol. Then, the resulting signal is integrated over T_{int}. This operation collects the contributions (that now are in phase) from several multipath components, but also contributions from noise and interference. The output of the integrator is the decision variable, the sign of which determines the bit estimate. The hybrid detector scheme is similar to the synchronization scheme proposed in [24] for preamble-based synchronization in OFDM systems and shares many of its advantages.

Mathematically speaking, we pass $r(t)$ through a receive filter matched to the following template signal for the ith information bit:

$$s_{temp}^{(i)}(t) = \frac{1}{\sqrt{N_f}} \sum_{j=iN_f}^{(i+1)N_f-1} d_j w_{rx}(t - jT_f - c_j T_c), \quad (3)$$

where $w_{rx}(t)$ is the received UWB pulse, which is usually modelled as the derivative of $w_{tx}(t)$ due to the effects of the antenna. For the analysis we assume that the received pulse shape is known and that the analog correlator is perfectly matched to the transmitted sequence of pulses. In case of mismatch, the autocorrelation function has to be adjusted accordingly later on in the analysis. The output of the matched filter can be expressed as

$$\tilde{r}(t) = \int r(\tau) s_{temp}^{(i)}(\tau - t) d\tau. \quad (4)$$

Since the receiver uses the despread signal $\tilde{r}(t)$, instead of $r(t)$, in the multiplication operation, the terms in the multiplication have a higher SNR, and the strong influence from the noise-noise terms can be decreased or almost eliminated. The SNR of the terms is increased by a factor N_f compared to the conventional TR scheme, where N_f is the number of monocycles per symbol. Note that the *effect* of that averaging is similar to averaging over several reference pulses as suggested in [8]; i.e., reducing the noise-noise cross-terms. However, when comparing the receiver *structure* to that of [8], we find important differences. The Choi/Stark receiver samples the signal at least once in each frame to allow the averaging of the reference pulses. The sampling, as well as the subsequent A/D conversion and digital processing of the sample values, thus occurs at the *frame* rate. Our scheme performs a filtering matched to the *transmit sequence*, followed by the multiplication, and sampling at the *data rate*. As the data rate is typically orders of magnitude lower than the frame rate, operating at such low rates allows large savings in the complexity and especially the power consumption of the transceiver.

The proposed receiver relies on that analog filters matched to the pulse sequence are available. These might, depending on the choice of parameters, be hard to realize since they require long analog delay lines with high reqirements on delay accuracy. It is anyway of interest to evaluate the performance of such a receiver structure to make it possible to judge whether it is worth, for the specific case, making some extra efforts in such analog correlators. Moreover, the proposed receiver structure provides an upper bound for the performance of conventional TR receivers, as will be investigated. The main difference from a conventional TR receiver, from a complexity point of view, is the analog matched filter. For the conventional receiver one still needs an analog delay and possibly the ability to make an average of the reference pulses. Also the conventional TR receiver requires frame-rate sampling, whereas the proposed receiver uses only symbol-rate samples. Therefore, the proposed receiver can be preferred for if the cost of the analog correlation operation can be compensated by low-rate sampling and high performance. In other words, throughput and cost requirements are important factors in selecting the type of the receiver.

III. Transmission over AWGN Channels

When $s_{TX}(t)$ in (1) is transmitted over an AWGN channel, the received signal can be expressed as

$$r(t) = \sqrt{\frac{E_s \alpha}{2N_f}} \sum_{j=-\infty}^{\infty} d_j [w_{rx}(t - jT_f - c_j T_c) + b_{\lfloor j/N_f \rfloor} w_{rx}(t - jT_f - c_j T_c - T_d)] + \sigma_n n(t), \quad (5)$$

where α is the channel attenuation, and $n(t)$ is a zero mean white Gaussian process with unit spectral density. Depending on whether we consider a baseband or bandpass signal, $n(t)$

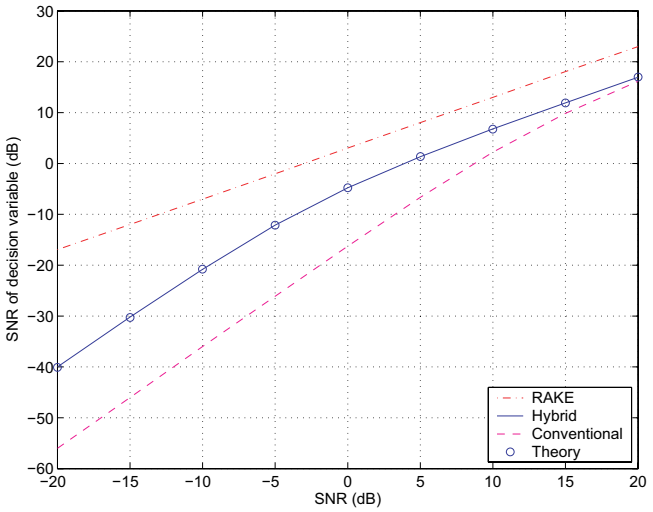

Fig. 2. SNR of the decision variable in AWGN, $N_f = 40$.

is a real or complex Gaussian process, respectively. The estimator in the AWGN case can be expressed as

$$\hat{b}_i = \text{sign}\{\tilde{r}(0)\tilde{r}(T_d)\}, \tag{6}$$

where $\tilde{r}(t)$ is the output of the matched filter as shown in (4). Of course, in practice one would not use this receiver for an AWGN channel, but this scenario serves as a benchmark and it is also used to explain some properties of the receiver. Note also that no integration is used in the AWGN case because there are no multipath components to combine.

The signal component of $\tilde{r}(0)\tilde{r}(T_d)$ is given as

$$\frac{E_s\alpha}{2}R^2(0)b_i, \tag{7}$$

where $R(t) = \int_{-\infty}^{\infty} w_{rx}(\tau)w_{rx}(\tau - t)d\tau$, while the energy of the signal-times-noise contribution is $E_s\alpha\sigma_n^2R^3(0)$, so that (without the noise-noise cross-terms), the SNR would be

$$\text{SNR} = \frac{E_s\alpha}{4\sigma_n^2}R(0). \tag{8}$$

This result can be easily explained intuitively: it is the SNR of an ideal Rake receiver, plus a 6 dB penalty. A 3 dB penalty arises from the fact that half of the signal energy is used for the reference pulse. The other half arises from the fact that the "local oscillator" is noisy, and actually contributes as much noise to the receiver output as the "desired signal". The SNR is further decreased (from its value of Eq. (8)) by the noise-noise cross-term, whose variance $\sigma_n^4R^2(0)$ is especially relevant at low SNRs. Fig. 2 plots the SNR of the decision variable in AWGN for different values of E_s/N_0 when using $N_f = 40$ frames per symbol for a coherent IR scheme, our proposed hybrid receiver and a correlating receiver without averaging of the reference pulses. For the hybrid receiver, the theoretical values of the SNR are also shown.

The effect of the noise-noise cross-terms can clearly be seen for low E_s/N_0. The breakpoint where these cross-terms become dominant is determined by N_f and is shifted towards low E_s/N_0 for a large N_f.

It is important to note that the noise-noise cross-terms do not have Gaussian statistics. Rather, they are the product of two Gaussian random variables, so that their probability density function (pdf) is given by [25]:

$$p_x(x) = \frac{1}{\pi\sigma^2}K_0\left(\frac{|x|}{\sigma^2}\right), \tag{9}$$

where $K_0(x)$ is the modified Bessel function zero-th order, second kind [26], and σ^2 is the variance of the underlying Gaussian process. Note that the structure of this noise is different from the one occurring in [8]. The total noise contribution consists thus of the sum of statistically dependent Gaussian and Bessel-distributed terms.

The following lemma expresses the exact probability distribution of the decision variable under some conditions.

Lemma 3.1: Assume that the TH sequence is constrained to the set $\{0, 1, \ldots, N_m - 1\}$, where $N_m = N_c - \Delta - 1$, with $\Delta = T_d/T_c$ being an integer. Then, the decision variable can be expressed as

$$\tilde{r}(0)\tilde{r}(T_d) = b_iR^2(0)\frac{E_s\alpha}{2} + N, \tag{10}$$

where the conditional distribution of N given the information bit b_i is given by

$$p_N(n|b_i) = \frac{1}{2\pi\sigma_n^2R(0)}\int_{-\infty}^{\infty}\frac{1}{|z + cb_i|} \cdot \exp\left\{-\frac{1}{2\sigma_n^2R(0)}\left[\frac{(n - cz)^2}{(z + cb_i)^2} + z^2\right]\right\}dz, \tag{11}$$

with $c = \sqrt{\frac{E_s\alpha}{2}}R(0)$.

Proof: See Appendix A.

For equiprobable information bits, the bit error probability (BEP) can be calculated from (10) as

$$P_e = 0.5\int_{-\infty}^{0} p_N\left(n - 0.5\alpha E_sR^2(0)\,|\,b_i = +1\right)dn + 0.5\int_{0}^{\infty} p_N\left(n + 0.5\alpha E_sR^2(0)\,|\,b_i = -1\right)dn.$$

Then, from (11), the following BEP expression can be obtained, after some manipulation, as

$$P_e = \frac{1}{\sqrt{2\pi R(0)\sigma_n^2}} \cdot \int_{-\infty}^{\infty} e^{-\frac{z^2}{2\sigma_n^2R(0)}}Q\left(\frac{cz + 0.5\alpha E_sR^2(0)}{\sqrt{R(0)\sigma_n^2}\,|z + c|}\right)dz, \tag{12}$$

where $Q(x) = \frac{1}{\sqrt{2\pi}}\int_x^{\infty} e^{-t^2/2}dt$.

Fig. 3 shows the simulation results for a TR scheme using $N_f = 40$, and compares them to the evaluations of (12). The results are in a very good agreement. Also the performance of the optimum receiver is plotted as a benchmark performance criterion.

IV. Transmission over Frequency-Selective Channels

For all practical purposes, IR systems always operate in frequency-selective channels. The high time resolution of the system ensures that different multipath components can be resolved very well. As a matter of fact, this fine resolution, and the associated high degree of delay diversity, is one of

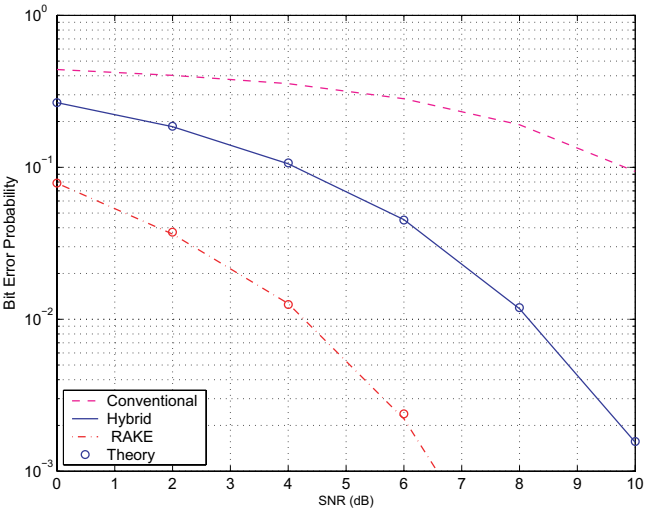

Fig. 3. BEP as a function of the signal-to-noise ratio for optimum (Rake) receiver, the hybrid receiver and the conventional receiver, $N_f = 40$. Solid curves are the Monte Carlo simulations, and the curves with circle marks are the theoretical results; i.e., evaluation of (12). The Monte Carlo simulations and the theoretical curves completely overlap.

the major advantages of UWB systems. It is thus necessary to analyze the performance of our receiver in frequency-selective channels.

A. Channel Model

The following channel model is considered [27]

$$h(t) = \sum_{l=0}^{L-1} a_l \delta(t - lT_r), \tag{13}$$

where L is the number of multipath components, T_r is the channel resolution ($T_r \leq T_c$) and a_l is the fading coefficient of the lth path. The channel is assumed to be normalized; that is, $\sum_{l=0}^{L-1} a_l^2 = 1$. Note that this model is completely general, as long as $1/T_r$ corresponds to at least the Nyquist sampling rate. Propagation channel models with random arrival times (e.g., [28], [23]) can be resampled and represented in the form (13) for any given system bandwidth. Even a chip-spaced channel model $1/T_r = 1/T_c$, with $1/T_r$ smaller than the Nyquist frequency, is a good representation of a general channel, and further simulations (not shown here) have shown only small deviations of the BER compared to the case of oversampled models.

The following assumptions are made in order to facilitate the theoretical analysis:

- The TH sequence c_j in (1) is constrained to the set $\{0, \ldots, N_m - 1\}$, where $N_m = N_c - Q - 1$, with Q being a positive integer determining the integration interval as explained later in this section.
- There is a guard interval between the symbols so that no inter-symbol interference (ISI) exists.

However, we stress that IFI, as well as interference from the reference pulses to the data pulses, is possible. This is an important generalization compared to [8].

B. General Theory

The received signal can be expressed, from (1) and (13), as

$$r(t) = \sqrt{\frac{E_s \alpha}{2N_f}} \sum_{j=-\infty}^{\infty} \sum_{l=0}^{L-1} a_l d_j [w_{rx}(t - jT_f - c_j T_c - lT_r) + b_{\lfloor j/N_f \rfloor} w_{rx}(t - jT_f - c_j T_c - T_d - lT_r)] + \sigma_n n(t). \tag{14}$$

From $r(t)$ in (14) and the template signal in (3), the despread signal $\tilde{r}(t)$ in (4) can be expressed, for the ith symbol, as

$$\tilde{r}(t) = \sqrt{\frac{E_s \alpha}{2N_f^2}} f_{b_i}(t) + \sigma_n n_w(t), \tag{15}$$

where

$$f_{b_i}(t) = \sum_{j=iN_f}^{(i+1)N_f - 1} \sum_{j'=iN_f}^{(i+1)N_f - 1} \sum_{l=0}^{L-1} a_l d_j d_{j'} \{R(t + (j' - j)T_f + (c_{j'} - c_j)T_c - lT_r) + b_i R(t + (j' - j)T_f + (c_{j'} - c_j)T_c - T_d - lT_r)\} \tag{16}$$

and

$$n_w(t) = \int_{-\infty}^{\infty} s_{temp}^{(i)}(\tau - t) n(\tau) d\tau, \tag{17}$$

with $s_{temp}^{(i)}(t)$ as in (3).

Although the expressions seem complex, (15) basically expresses the output of the analog match-filtering in Fig. 1 as the summation of a signal and a noise term. Then, the information bit is estimated as the sign of the integral of the multiplication between the despread signal and its delayed version:

$$\hat{b}_i = \text{sign}\{\xi(t)\} = \text{sign}\left\{ \int_{T_d - T_c}^{T_d + QT_c} \tilde{r}(t)\tilde{r}(t - T_d) dt \right\}, \tag{18}$$

where Q is an integer that determines the integration interval. Note that the detection algorithm is basically the conventional delay-and-multiply operation applied on the despread signal $\tilde{r}(t)$. In this case, the decision variable can be expressed as

$$\xi(t) = \int_{T_d - T_c}^{T_d + QT_c} \tilde{r}(t)\tilde{r}(t - T_d) dt = S + N_1 + N_2, \tag{19}$$

where S is the desired signal part, N_1 is the noise-noise term and N_2 is the signal-noise term, the closed form of which can be found in Appendix B. Note that the noise terms N_1 and N_2 are uncorrelated random variables.

Using these results, the BEP can now be expressed as

$$P_e = 0.5\, Q\left(\frac{0.5 E_s \alpha \int_{T_d - T_c}^{T_d + QT_c} f_{+1}(t) f_{+1}(t - T_d) dt}{N_f \sqrt{\sigma_n^4 (Q+1) N_f^2 \sigma_1^2 + 0.5 \sigma_n^2 E_s \alpha\, \sigma_2^2(1)}} \right) + 0.5\, Q\left(\frac{-0.5 E_s \alpha \int_{T_d - T_c}^{T_d + QT_c} f_{-1}(t) f_{-1}(t - T_d) dt}{N_f \sqrt{\sigma_n^4 (Q+1) N_f^2 \sigma_1^2 + 0.5 \sigma_n^2 E_s \alpha\, \sigma_2^2(-1)}} \right), \tag{20}$$

where σ_1^2 and $\sigma_2^2(b_i)$ are given in Appendix B.

The special case of no IFI makes it possible to simplify the terms in this expression, the details of which can be found in Appendix C.

C. Optimal Integration Interval

For a given TR system, the integration interval needs to be optimized in order to minimize the BEP [29], [30]. The approximate BEP expression in (20) can be used to obtain an optimal integration interval, equivalently Q in (18), for that purpose.

For the case of no IFI and no interference between the reference and the data pulses, a simpler expression can be obtained for optimal Q values assuming a chip-spaced channel model ($T_r = T_c$). After some manipulation, $\sigma_2^2(b_i)$ in (48) can be expressed, from (46), (50) and (3), as

$$\sigma_2^2(b_i) = \tag{21}$$
$$N_f^3 \int_{-\infty}^{\infty} \left\{ \begin{array}{c} \int_{-T_c}^{QT_c} \sum_{l=0}^{L-1} a_l R(t - lT_c) \\ \cdot [s_{temp}(\tau - t - T_d) + b_i s_{temp}(\tau - t)] dt \end{array} \right\}^2 d\tau,$$

which can be reduced to

$$\sigma_2^2(b_i) = 2N_f^3 \int_{-T_c}^{QT_c} \int_{-T_c}^{QT_c} I(t_1, t_2) dt_1 dt_2, \tag{22}$$

where

$$I(t_1, t_2) = R(t_2 - t_1) \sum_{l_1=0}^{L-1} \sum_{l_2=0}^{L-1} a_{l_1} a_{l_2} R(t_1 - l_1 T_c) R(t_2 - l_2 T_c).$$

Note that $\sigma_2^2(b_i)$ is independent of the information bit b_i in this case. Therefore, the optimal Q value can be calculated, from (19), (58), (47) and (22), as follows:

$$Q_{opt} = \arg\max_{Q} \tag{23}$$
$$\left\{ \frac{0.5 E_s \alpha \sum_{q=0}^{Q} [A(a_{q-1}^2 + a_q^2) + 2C a_{q-1} a_q]}{\sqrt{\sigma_n^4 \sigma_1^2 (Q+1) + \sigma_n^2 E_s \alpha N_f \int_{-T_c}^{QT_c} \int_{-T_c}^{QT_c} I(t_1, t_2) dt_1 dt_2}} \right\}.$$

In order to get a simpler expression in the limiting case of very narrow UWB pulses, consider a pulse shape of an impulse function. Then, $\sigma_2^2(b_i)$ becomes

$$\sigma_2^2(b_i) = 2N_f^3 E_R R(0) \sum_{q=0}^{Q} a_q^2, \tag{24}$$

and the signal part becomes $0.5 E_s E_R \alpha \sum_{q=0}^{Q} a_q^2$, where $E_R = \int_{-\infty}^{\infty} R^2(t) dt$. Hence, the optimal Q can be obtained as follows:

$$Q_{opt} = \arg\max_{Q} \tag{25}$$
$$\left\{ \frac{0.5 E_s E_R \alpha \sum_{q=0}^{Q} a_q^2}{\sqrt{\sigma_n^4 \sigma_1^2 (Q+1) + \sigma_n^2 E_s E_R R(0) \alpha N_f \sum_{q=0}^{Q} a_q^2}} \right\}.$$

Note that if the noise-noise term, the first term in the denominator, is negligible, then it is always better to integrate over more multipath components. However, if the noise-noise term is not negligible, there can be a certain Q value, after which it is worse to combine more multipath components, since addition of noise-noise terms becomes more effective than the desired signal component at that point. When the noise-noise term is very large compared to the signal-noise term, the optimal Q value is approximately given by

$$Q_{opt} = \arg\max_{Q} \left\{ \frac{1}{\sqrt{Q+1}} \sum_{q=0}^{Q} a_q^2 \right\}. \tag{26}$$

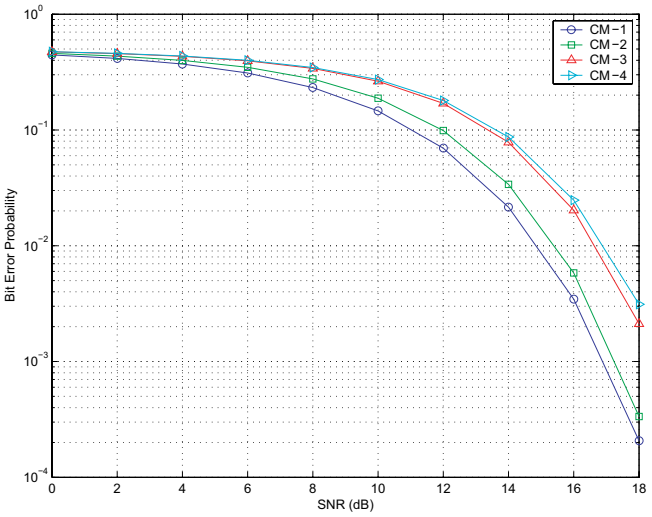

Fig. 4. BEP versus SNR for different IEEE channel models. The parameters are $N_f = 3$, $N_c = 100$ and $\Delta = 50$. $Q = 10, 20, 50, 50$ for CM-1, CM-2, CM-3 and CM-4, respectively. Average BEPs are obtained by means of averaging over 100 channel realizations for each model.

V. Performance Evaluation

In this section, we perform computer simulations in order to study the properties of the proposed hybrid system and verify the theoretical analysis.

In the simulations, we have considered channel models from the IEEE 802.15.3a standard [23]. Those channel models, which were designed for 7.5 GHz bandwidth, are bandpass filtered for a simulation of a 500 MHz wide system. The polarity codes and the TH codes are randomly generated from the sets $\{-1, +1\}$ and $\{0, 1, 2\}$, respectively[2].

Fig. 4 plots the theoretical BEP curves versus SNR for the four different IEEE channel models, CM-1, CM-2, CM-3 and CM-4. For each channel, the integration interval (equivalently Q in (18)) is roughly optimized and the systems are simulated with those optimal Q values. The number of frames per symbol, N_f, is 3, the number of chips per frame, N_c, is 100 and the chip duration T_c is 2 ns. The distance between the reference and the date pulse is 50 chips; that is, $\Delta = 50$. From the figure, it is observed that the performance gets worse from CM-1 to CM-4 since the channel delay spread gets larger, which increases the effects of the IFI and reference-to-data pulse interference.

In Fig. 5, $N_c = 25$, $N_f = 10, T_c = 2$ ns and $\Delta = 12$ are used in CM-1, and the theoretical and simulation results are compared for the conventional receiver and the hybrid receiver for different values of Q. We observe that as Q increases the theoretical and simulation results get closer. This is expected since the approximate BEP expression is derived under the

[2]Since we consider a single-user system, the TH code is generated from a small set for convenience. In fact, the analysis holds for any value of the TH code from the set $\{0, 1, \ldots, N_c - Q - 2\}$.

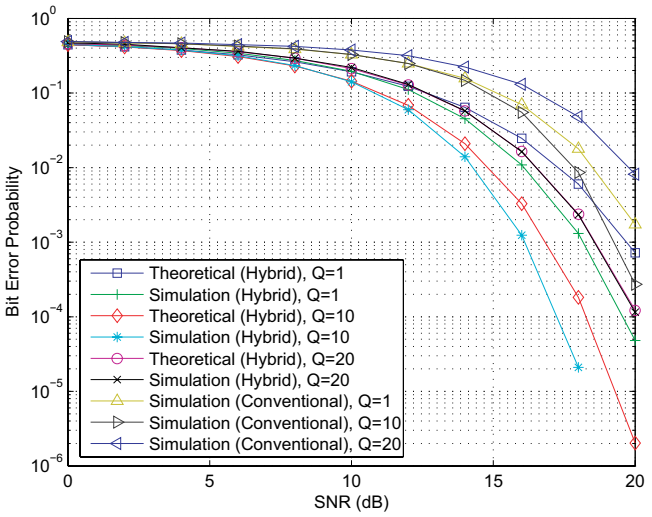

Fig. 5. BEP versus SNR for the conventional receiver and the hybrid receiver for different Q values. $N_c = 25$, $N_f = 10$ and $\Delta = 12$ and a realization of CM-1 is employed.

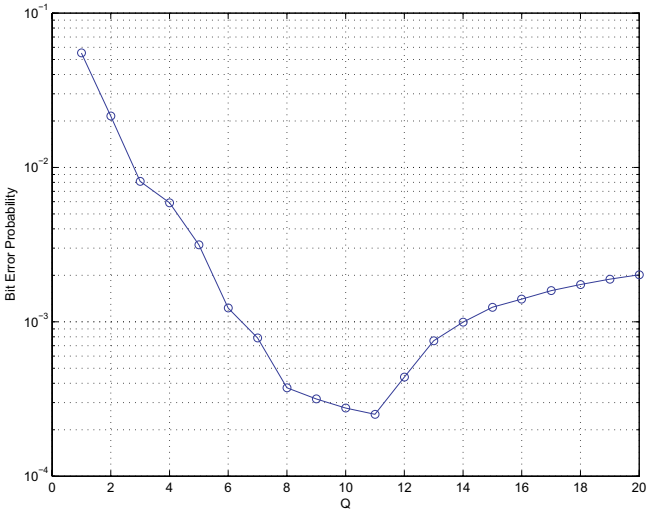

Fig. 6. BEP versus Q at SNR $= 18$ dB. $N_c = 25$, $N_f = 10$ and $\Delta = 12$ are used, and averaging over 100 realizations of CM-1 is performed. The optimal value is $Q = 11$.

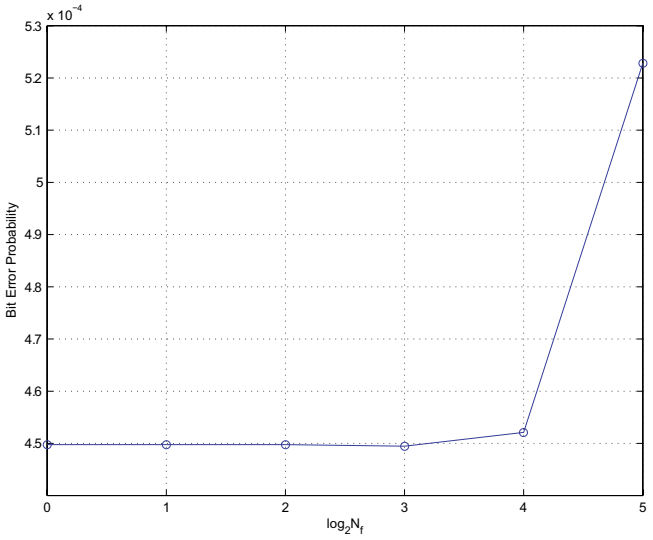

Fig. 7. BEP versus N_f at SNR $= 18$ dB. The parameters are $Q = \Delta = 12$ and $N_c N_f = 512$, and CM-1 is considered.

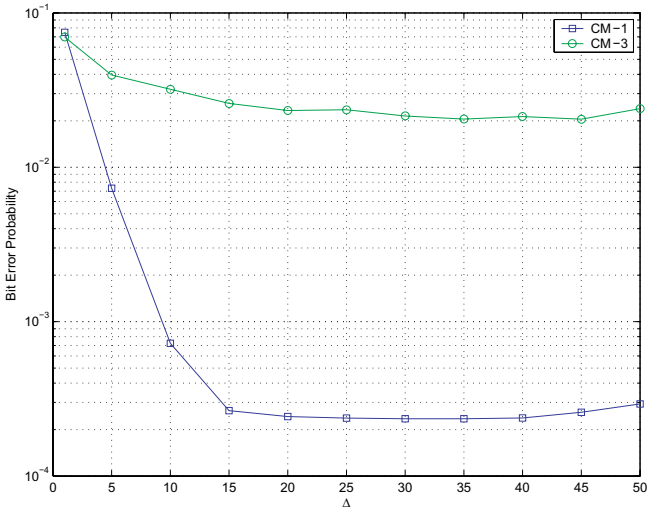

Fig. 8. BEP versus Δ at SNR $= 18$ dB. $N_c = 50$ and $N_f = 6$ are used and BEP is averaged over 100 realizations of CM-1 and CM-3.

condition of large Q values; that is, Lemma 1.1 states that the noise-noise term converges in distribution to a Gaussian random variable as $Q \longrightarrow \infty$. We here see clearly that the hybrid receiver outperforms the conventional TR receiver.

Using the same parameters as in the previous case, we plot, in Fig. 6, the BEP performance of the system in CM-1 for different Q values at SNR $= 18$ dB. From the figure, we deduce that for small Q values, the integration interval is small and therefore very little signal energy is collected. As Q increases to larger values, more signal energy is collected, hence the BEP decreases. However, after a certain point, the collected signal energy becomes less significant than the collected noise-noise and/or interference terms. Therefore, the BEP increases as we increase Q further. From the figure, the optimal value is observed to be at $Q = 11$.

For the next simulations, $Q = \Delta = 12, T_c = 2$ ns, SNR $=$ 18 dB and the number of chips per symbol is 512; that is $N_c N_f = 512$. For a fixed symbol time and energy, the number of frames per symbol is varied and the BEP is plotted in Fig. 7 for CM-1. From the plot, it is observed that the frame size does not matter up to the point where IFI becomes dominant. After the frame duration is 16 chips ($N_c = 16$), and thus the IFI becomes significant (due to $\Delta = 12$ and the channel spread), the BEP increases.

For the final simulations, $N_c = 50$, $N_f = 6, T_c = 2$ ns and SNR $= 18$ dB. Fig. 8 plots the BEP versus Δ, which is the distance in chips between the reference pulse and the data pulse. As observed from the figure, for small values of Δ, the BEP is high due to the severe interference between the reference and the data pulses. For very large Δ, the BEP is also high since the IFI becomes dominant in that case. Therefore, the optimal value should minimize the total effects of the interference between the reference and data pulses and the pulses from different frames.

VI. Conclusions

In this paper we have analyzed a hybrid matched-filter TR correlation receiver. The proposed receiver performs matched filter detection before correlating (multiplying) the data symbol with the reference symbol. Therefore the SNR in this multiplication operation is much better compared to the SNR in the corresponding multiplication for the conventional TR receiver, and the proposed receiver does not suffer from large noise-noise terms. After the multiplication, the signals from different multipath components have the same phase and therefore they can be integrated to capture signal energy from the whole, or a large portion of, the impulse response. We have found that the impact of the non-Gaussian nature of the noise on the BEP can be significant, and given exact closed-form equations for both the resulting variance and the average BEP. We have then analyzed the BEP performance in multipath environments. Lifting restrictions of previous treatments of the topic, we have included the effect of IFI as well as interference between the reference pulse and the data pulse.

Including the effects of IFI is crucial for optimizing the receiver design of TR systems. Requiring frame durations that are larger than the maximum excess delay of the channel severely restricts the frame rate, and thus the processing gain due to multiple frames, in a TH-IR system. Extremely long frame durations also mean that the peak-to-average ratio of the transmit signal becomes high, which is undesirable both from a hardware point of view, and from a frequency-regulation point of view (note that the FCC report and order [1] limits the admissible peak-to-average ratio).

It is also important to consider the case that the delay between the data pulse and the reference pulse is smaller than the maximum excess delay of the channel. In many systems, the delay in the receiver is implemented by delay lines. However, it is not straightforward to build delay lines on the order of 10-100 ns (typical values for channel maximum excess delays). Therefore, interference between reference pulse and data pulse will occur in practice.

The results of our paper are thus important tools for system design and computation performance of TR IR systems with practically relevant operating parameters.

Appendix

A. Proof of Lemma 3.1

The despread signal $\tilde{r}(t)$ is the convolution of the template signal in (3) and the received signal in (5), as shown in (4). Therefore, the decision variable can be calculated as

$$\tilde{r}(0)\tilde{r}(T_d) = \left(\sqrt{\frac{E_s\alpha}{2N_f^2}}\sum_{j=iN_f}^{(i+1)N_f-1}[R(0)+b_{\lfloor j/N_f\rfloor}R(-T_d)]+n_w(0)\right) \cdot\left(\sqrt{\frac{E_s\alpha}{2N_f^2}}\sum_{j=iN_f}^{(i+1)N_f-1}[R(T_d)+b_{\lfloor j/N_f\rfloor}R(0)]+n_w(T_d)\right), \tag{27}$$

with $n_w(t)$ given by

$$n_w(t)=\frac{\sigma_n}{\sqrt{N_f}}\sum_{j=iN_f}^{(i+1)N_f-1}d_j\int n(\tau)w_{rx}(\tau-t-jT_f-c_jT_c)d\tau.$$

The assumption in the lemma makes sure that no data pulse overlaps with the reference pulse in the next frame. Therefore, it can be shown that $n_w(0)$ and $n_w(T_d)$ are uncorrelated, hence independent due to the Gaussian nature. Also using the fact that $T_d \geq T_c$ and that $R(x)=0$ for $|x|\geq T_c$, we get

$$\tilde{r}(0)\tilde{r}(T_d) = b_iR^2(0)\frac{E_s\alpha}{2}+N, \tag{28}$$

where

$$N=\sqrt{\frac{E_s\alpha}{2}}R(0)(b_iX+Y)+XY, \tag{29}$$

with $X=n_w(0)$ and $Y=n_w(T_d)$.

In order to obtain the probability distribution of N, we first define the mapping from (X,Y) to (N,M) as

$$N=c(b_iX+Y)+XY, \tag{30}$$

$$M=Y, \tag{31}$$

where $c=\sqrt{\frac{E_s\alpha}{2}}R(0)$. Then, the inverse transform can be expressed as

$$X=\frac{N-cM}{M+b_ic}, \tag{32}$$

$$Y=M. \tag{33}$$

Using the fact that $p_{X,Y}(x,y)=\frac{1}{2\pi\sigma^2}e^{-(x^2+y^2)/(2\sigma^2)}$ with $\sigma^2=\sigma_n^2R(0)$ and obtaining the absolute value of the determinant of the Jacobian as

$$|J(n,m)|=\begin{vmatrix}\frac{1}{m+b_ic} & -\frac{n+b_ic^2}{(m+b_ic)^2}\\ 0 & 1\end{vmatrix}=\frac{1}{|m+b_ic|}, \tag{34}$$

we get [31]

$$p_{N,M}(n,m|b_i)=\frac{1}{|m+b_ic|}\;p_{X,Y}\left(\frac{n-cm}{m+b_ic},m\right) \tag{35}$$

$$=\frac{1}{2\pi\sigma^2}\frac{1}{|m+b_ic|}\exp\left\{-\frac{1}{2\sigma^2}\left[\frac{(n-cm)^2}{(m+b_ic)^2}+m^2\right]\right\}.$$

Then, from the relation, $p_N(n|b_i)=\int_{-\infty}^{\infty}p_{N,M}(n,m|b_i)dm$, we obtain $p_N(n|b_i)$ as in (11). □

B. Distribution of noise terms

From (15), the signal part S of the decision variable in (19) can be expressed as

$$S = \frac{E_s \alpha}{2N_f^2} \int_{T_d - T_c}^{T_d + QT_c} f_{b_i}(t) f_{b_i}(t - T_d) dt, \tag{36}$$

where $f_{b_i}(t)$ is as in (16). Note that S is basically the autocorrelation of the signal part of the despread signal $\tilde{r}(t)$ in (15). Similarly, the noise-noise term N_1 in (19) can be obtained from (15) as

$$N_1 = \sigma_n^2 \int_{T_d - T_c}^{T_d + QT_c} n_w(t) n_w(t - T_d) dt, \tag{37}$$

the distribution of which can be approximated as shown in the following lemma:

Lemma 1.1: As $Q \longrightarrow \infty$, $N_1/\sqrt{Q+1}$ is asymptotically normally distributed as

$$\mathcal{N}\left(0\,,\, \sigma_n^4 \int_{-\infty}^{\infty} \int_{-\infty}^{\infty} [l_q^2(\tau, \hat{\tau}) + 2 l_q(\tau, \hat{\tau}) l_{q+1}(\tau, \hat{\tau})] d\tau d\hat{\tau}\right), \tag{38}$$

where

$$l_q(\tau, \hat{\tau}) = \int_{T_d + (q-1)T_c}^{T_d + qT_c} s_{temp}^{(i)}(\tau - t) s_{temp}^{(i)}(\hat{\tau} - t + T_d) dt. \tag{39}$$

Proof:

N_1 in (37) can be expressed as $N_1 = \sigma_n^2 \sum_{q=0}^{Q} N_{1,q}$ where

$$N_{1,q} = \int_{T_d + (q-1)T_c}^{T_d + qT_c} n_w(t) n_w(t - T_d) dt. \tag{40}$$

From (17), $N_{1,q}$ can be expressed as

$$N_{1,q} = \int_{-\infty}^{\infty} \int_{-\infty}^{\infty} n(\tau_1) n(\tau_2) \cdot \int_{T_d + (q-1)T_c}^{T_d + qT_c} s_{temp}^{(i)}(\tau_1 - t) s_{temp}^{(i)}(\tau_2 - t + T_d)\, dt\, d\tau_1\, d\tau_2, \tag{41}$$

where $s_{temp}^{(i)}(t)$ is as in (3).

It can be shown that $\{N_{1,q}\}_{q=0}^{Q}$ are identically distributed and form a 1-dependent sequence, since the $N_{1,q}$ and $N_{1,r}$ become independent for $|q - r| > 1$. This is because the sets of τ_1 and τ_2, for which the innermost integral is non-zero, are disjoint for $|q - r| > 1$, and the result follows since $n(t)$ is a white Gaussian noise process. Since $\{N_{1,q}\}_{q=0}^{Q}$ form a 1-dependent sequence, (38) and (39) can be evaluated for any q in $[0, Q]$.

From the first assumption in Section IV-A, it can be shown after some manipulation that $\mathrm{E}\{N_{1,q}\} = 0$ and

$$\mathrm{E}\{N_{1,q}^2\} = \int_{-\infty}^{\infty} \int_{-\infty}^{\infty} l_q^2(\tau, \hat{\tau}) d\tau d\hat{\tau}, \tag{42}$$

where $l_q(\tau, \hat{\tau})$ is as in (39). Similarly, the correlation term can be obtained as

$$\mathrm{E}\{N_{1,q} N_{1,q+1}\} = \int_{-\infty}^{\infty} \int_{-\infty}^{\infty} l_q(\tau, \hat{\tau}) l_{q+1}(\tau, \hat{\tau}) d\tau d\hat{\tau}. \tag{43}$$

Using the central-limit argument for 1-dependent sequences [32], the asymptotic distribution of the noise-noise term, as $Q \longrightarrow \infty$, is obtained as

$$\frac{1}{\sqrt{Q+1}} \sum_{q=0}^{Q} N_{1,q} \sim \mathcal{N}\left(0\,,\, \mathrm{E}\{N_{1,q}^2\} + 2\mathrm{E}\{N_{1,q} N_{1,q+1}\}\right),$$

from which (38) follows, using (42) and (43). □

Note that Lemma 1.1 states that when the integration interval is large, the noise-noise term is approximately a zero mean Gaussian random variable.

From (15), the signal-noise term N_2 in (19) is obtained as

$$N_2 = \sqrt{\frac{E_s \alpha \sigma_n^2}{2N_f^2}} \int_{T_d - T_c}^{T_d + QT_c} [f_{b_i}(t) n_w(t - T_d) + n_w(t) f_{b_i}(t - T_d)] dt. \tag{44}$$

From (17) and the fact that $n(t)$ is a white Gaussian process, we observe that N_2 is a Gaussian random variable since it is a weighted integral of $n(t)$. After some manipulation, it can be shown that

$$N_2 \sim \mathcal{N}\left(0\,,\, \frac{\sigma_n^2 E_s \alpha}{2N_f^2} \int_{-\infty}^{\infty} [h_{b_i}(\tau; 0, T_d) + h_{b_i}(\tau; T_d, 0)]^2 d\tau\right), \tag{45}$$

where

$$h_{b_i}(\tau; x, y) = \int_{T_d - T_c}^{T_d + QT_c} f_{b_i}(t - x) s_{temp}^{(i)}(\tau - t + y) dt. \tag{46}$$

Now consider the total noise $N = N_1 + N_2$. It can be shown from (37) and (44) that, N_1 and N_2 are uncorrelated because of the structure of the noise $n_w(t)$ in (17) and short UWB pulse durations. Hence, the approximate distribution of the total noise N can be obtained from (38) and (45) as

$$N \sim \mathcal{N}\left(0\,,\, \sigma_n^4 (Q+1) \sigma_1^2 + \frac{\sigma_n^2 E_s \alpha}{2N_f^2} \sigma_2^2(b_i)\right), \tag{47}$$

where

$$\sigma_1^2 = \int_{-\infty}^{\infty} \int_{-\infty}^{\infty} [l_q^2(\tau, \hat{\tau}) + 2 l_q(\tau, \hat{\tau}) l_{q+1}(\tau, \hat{\tau})] d\tau d\hat{\tau}, \tag{48}$$

$$\sigma_2^2(b_i) = \int_{-\infty}^{\infty} [h_{b_i}(\tau; 0, T_d) + h_{b_i}(\tau; T_d, 0)]^2 d\tau. \tag{49}$$

C. Special Case: BEP with no Inter-frame Interference

When the frame intervals are sufficiently large and the TH sequence is constrained in a certain interval, there can occur no IFI in the system. However, there can still be interference from the reference pulses to the data pulses, as those are typically spaced more closely. In the case of no IFI, we can obtain simple expressions for BEP for a chip-spaced channel model ($T_r = T_c$).

Assume that $N_m \leq N_c - \Delta - \max\{Q, L\}$. Then, $f_{b_i}(t)$ in (16) can be expressed as follows:

$$f_{b_i}(t) = N_f \sum_{l=0}^{L-1} a_l [R(t - lT_c) + b_i R(t - (\Delta + l)T_c)]. \tag{50}$$

Hence, the signal part in (36) can be expressed

$$S = \frac{E_s \alpha}{2}[(S_1 + S_2) + b_i(S_3 + S_4)], \tag{51}$$

where S_1, S_2, S_3 and S_4 can be shown to be given by

$$\begin{aligned} S_1 = \sum_{q=0}^{Q} [&A(a_{q-1}a_{q+\Delta-1} + a_q a_{q+\Delta}) \\ &+ C(a_q a_{q+\Delta-1} + a_{q-1}a_{q+\Delta})], \end{aligned} \tag{52}$$

$$\begin{aligned} S_2 = \sum_{q=0}^{Q} [&A(a_{q-1}a_{q-\Delta-1} + a_q a_{q-\Delta}) \\ &+ C(a_{q-1}a_{q-\Delta} + a_q a_{q-\Delta-1})], \end{aligned} \tag{53}$$

$$\begin{aligned} S_3 = \sum_{q=0}^{Q} [&A(a_{q+\Delta-1}a_{q-\Delta-1} + a_{q+\Delta} a_{q-\Delta}) \\ &+ C(a_{q+\Delta-1}a_{q-\Delta} + a_{q+\Delta}a_{q-\Delta-1})], \end{aligned} \tag{54}$$

$$S_4 = \sum_{q=0}^{Q} [A(a_{q-1}^2 + a_q^2) + 2C(a_{q-1}a_q)], \tag{55}$$

where $A = \int_0^{T_c} R^2(t)dt = \int_{-T_c}^{0} R^2(t)dt$ and $C = \int_0^{T_c} R(t)R(t+T_c)dt$. Note that $a_l = 0$ for $l > L-1$ or $l < 0$.

From (52)-(55) $S_1 + S_2$ and $S_3 + S_4$ can be expressed as

$$\begin{aligned} S_1 + S_2 = \sum_{q=0}^{Q} [&(a_{q+\Delta} + a_{q-\Delta})(Aa_q + Ca_{q-1}) \\ &+ (a_{q+\Delta-1} + a_{q-\Delta-1})(Aa_{q-1} + Ca_q)], \end{aligned} \tag{56}$$

$$\begin{aligned} S_3 + S_4 = &\\ \sum_{q=0}^{Q} [&A(a_{q-1}^2 + a_q^2 + a_{q+\Delta-1}a_{q-\Delta-1} + a_{q+\Delta}a_{q-\Delta}) \\ &+ C(2a_{q-1}a_q + a_{q+\Delta-1}a_{q-\Delta} + a_{q+\Delta}a_{q-\Delta-1})]. \end{aligned} \tag{57}$$

Note that when $\Delta > L > Q$, the signal part in (36) can be expressed as

$$S = b_i \frac{E_s \alpha}{2} \sum_{q=0}^{Q} [A(a_{q-1}^2 + a_q^2) + 2C(a_{q-1}a_q)], \tag{58}$$

which corresponds to the case that no collision occurs between the reference and the data pulse.

The noise term $N = N_1 + N_2$ can be shown to be distributed as in (47), where $\sigma_2^2(b_i)$ in (49) is now given by

$$\sigma_2^2(b_i) = \int_{-\infty}^{\infty} [h_{b_i}^2(\tau; 0, T_d) + h_{b_i}^2(\tau; T_d, 0)]d\tau. \tag{59}$$

Then, the BEP expression is obtained as

$$\begin{aligned} P_e = &0.5\, Q\left(\frac{0.5E_s\alpha(S_1 + S_2 + S_3 + S_4)}{\sqrt{\sigma_n^4(Q+1)\,\sigma_1^2 + \frac{\sigma_n^2 E_s \alpha}{2N_f^2}\,\sigma_2^2(1)}} \right) \\ &+ 0.5\, Q\left(\frac{0.5E_s\alpha(S_3 + S_4 - S_1 - S_2)}{\sqrt{\sigma_n^4(Q+1)\,\sigma_1^2 + \frac{\sigma_n^2 E_s \alpha}{2N_f^2}\,\sigma_2^2(-1)}} \right). \end{aligned} \tag{60}$$

REFERENCES

[1] Federal Communications Commission, "First Report and Order 02-48," 2002.

[2] R. A. Scholtz, "Multiple access with time-hopping impulse modulation," in *Proc. IEEE Military Communications Conference (MILCOM'93)*, vol. 2, pp. 447-450.

[3] M. Z. Win and R. A. Scholtz, "Ultra-wide bandwidth time-hopping spread-spectrum impulse radio for wireless multiple-access communications," *IEEE Trans. Commun.*, vol. 48, pp. 679-691, Apr. 2000.

[4] IEEE 802.15 WPAN Low Rate Alternative PHY Study Group 4a (SG4a) (online), available at: http://www.ieee802.org/15/pub/SG4a.html

[5] M. Z. Win and R. A. Scholtz, "Impulse radio: how it works," *IEEE Commun. Lett.*, vol. 2, no. 2, pp. 36-38, Feb. 1998.

[6] M. Z. Win and R. A. Scholtz, "On the energy capture of ultra-wide bandwidth signals in dense multipath environments," *IEEE Commun. Lett.*, vol. 2, pp. 245-247, Sept. 1998.

[7] D. Cassioli, M. Z. Win, A. F. Molisch, and F. Vatelaro, "Performance of low-complexity RAKE reception in a realistic UWB channel," in *Proc. IEEE International Conference on Communications (ICC 2002)*, vol. 2, pp. 763-767.

[8] J. D. Choi and W. E. Stark, "Performance of ultra-wideband communications with suboptimal receivers in multipath channels," *IEEE J. Sel. Areas Commun.*, vol. 20, no. 9, pp. 1754-1766, Dec. 2002.

[9] H. Niu, J. A. Ritcey, and H. Liu, "Performance of UWB Rake receivers with imperfect tap weights," in *Proc. IEEE International Conference on Acoustics, Speech, and Signal Processing (ICASSP '03)*, vol. 4, pp. 125-128.

[10] H. Sheng, R. You, and A. M. Haimovich, "Performance analysis of ultra-wideband Rake receivers with channel delay estimation errors," in *Proc. 38th Annual Conference on Information Sciences and Systems (CISS'04)*, pp. 921-926.

[11] R. Hoctor and H. Tomlinson, "Delay-hopped transmitted-reference RF communications," in *Proc. IEEE Conference of Ultra Wideband Systems and Technologies 2002 (UWBST'02)*, pp. 265-269.

[12] L. Yang and G. B. Giannakis, "Optimal pilot waveform assisted modulation for ultrawideband communications," *IEEE Trans. Wireless Commun.*, vol. 3, no. 4, pp. 1236-1249, July 2004.

[13] M. Ho, V. S. Somayazulu, J. Foerster, and S. Roy, "A differential detector for an ultra-wideband communications system," in *Proc. IEEE Vehicular Technology Conference (VTC 2002 Spring)*, pp. 1896-1900.

[14] Y. L. Chao and R. A. Scholtz, "Optimal and suboptimal receivers for ultra-wideband transmitted reference systems," in *Proc. IEEE Global Telecommunications Conference (GLOBECOM'03)*, vol. 2, pp. 759-763.

[15] N. van Stralen, A. Dentinger, K. Welles II, R. Gaus Jr., R. Hoctor, and H. Tomlinson, "Delay hopped transmitted reference experimental results," in *Proc. IEEE Conference of Ultra Wideband Systems and Technologies 2002 (UWBST 2002)*, pp. 93-98.

[16] F. Dowla, F. Nekoogar, and A. Spiridon, "Interference mitigation in transmitted-reference ultra-wideband (UWB) receivers," in *Proc. IEEE Antennas and Propagation Society Symposium,* vol. 2, pp. 1307-1310.

[17] H. Zhang and D. L. Goeckel, "Generalized transmitted-reference UWB systems," in *Proc. IEEE Conference on Ultra Wideband Systems and Technologies (UWBST 2003)*, pp. 147-151.

[18] S. Franz and U. Mitra, "On optimal data detection for UWB transmitted reference systems," in *Proc. IEEE Global Telecommunications Conference (GLOBECOM'03)*, vol. 2, pp. 744-748.

[19] F. Tufvesson and A. F. Molisch, "Ultra-wideband communication using hybrid matched filter correlation receivers," in *Proc. IEEE Vehicular Technology Conference (VTC 2004 Spring)*, vol. 3, pp. 1290-1294.

[20] K. Witrisal, M. Pausini, and A. Trindade, "Multiuser interference and inter-frame interference in UWB transmitted reference systems," in *Proc. IEEE Conference on Ultra Wideband Systems and Technologies (UWBST 2004)*, pp. 96-100.

[21] J. G. Proakis, *Digital Communications, Fourth Edition*. McGraw Hill, 2000.

[22] Y.-P. Nakache and A. F. Molisch, "Spectral shape of UWB signals influence of modulation format, multiple access scheme and pulse shape," in *Proc. IEEE Vehicular Technology Conference, (VTC 2003-Spring)*, vol. 4, pp. 2510-2514.

[23] A. F. Molisch, J. R. Foerster, and M. Pendergrass, "Channel models for ultrawideband personal area networks," *IEEE Personal Commun. Mag.*, vol. 10, no. 6, pp. 14-21, Dec. 2003.

[24] F. Tufvesson, "Design of wireless communication systems: issues on synchronization, channel estimation and multi-carrier systems," Ph.D. Thesis, Lund University, Sweden, 2000.

[25] M. K. Simon, *Probability Distributions Involving Gaussian Random Variables*. Kluwer Academic Press, 2002.

[26] M. Abramowitz and I. Stegun, *Handbook of Mathematical Function, Second Edition*. New York: Dover, 1972.
[27] A. F. Molisch, *Wireless Communications*. IEEE-Press Wiley, 2005.
[28] A. Saleh and R. Valenzuela, "A statistical model for indoor multipath propagation," *IEEE J. Sel. Areas Commun.*, vol. 5, no. 2, pp. 128-137, Feb. 1987.
[29] S. Franz and U. Mitra, "Integration interval optimization and performance analysis for UWB transmitted reference systems," in *Proc. IEEE Conference on Ultra Wideband Systems and Technologies (UWBST 2004)*, pp. 26-30.
[30] T. Zasowski, F. Althaus, and A. Wittneben, "An energy efficient transmitted-reference scheme for ultra wideband communications," in *Proc. IEEE Conference on Ultra Wideband Systems and Technologies (UWBST 2004)*, pp. 146-150.
[31] A. Leon-Garcia, *Probability and Random Processes for Electrical Engineering, Second Edition*. Reading, MA: Addison-Wesley, 1994.
[32] P. Billingsley, *Probability and Measure, Second Edition.* New York: John Wiley & Sons, 1986.

Fredrik Tufvesson was born in Lund, Sweden in 1970. He received the M.S. degree in Electrical Engineering in 1994, the Licentiate Degree in 1998 and his Ph.D. in 2000, all from Lund University in Sweden. After almost two years at a startup company, Fiberless Society, Fredrik is now associate professor at the department of Electroscience. His main research interests are channel measurements and modeling for wireless communication, including channels for both MIMO and UWB systems. Beside this, he also works with channel estimation and synchronization problems, OFDM system design and UWB transceiver design.

Sinan Gezici received the B.S. degree from Bilkent University, Turkey in 2001, and the Ph.D. degree in Electrical Engineering from Princeton University in 2006. He is currently working as a Visiting Member of Technical Staff at Mitsubishi Electric Research Laboratories, Cambridge, MA.His main research interests are in the fields of signal detection, estimation and optimization theory, and their applications to wireless communication systems. Currently, he has a particular interest in timing estimation, performance analysis and receiver design for ultra-wideband systems.

Andreas F. Molisch (S'89, M'95, SM'00, F'05) received the Dipl. Ing., Dr. techn., and habilitation degrees from the Technical University Vienna (Austria) in 1990, 1994, and 1999, respectively. From 1991 to 2000, he was with the TU Vienna, becoming an associate professor there in 1999. From 2000-2002, he was with the Wireless Systems Research Department at AT&T (Bell) Laboratories Research in Middletown, NJ. Since then, he has been a Senior Principal Member of Technical Staff with Mitsubishi Electric Research Labs, Cambridge, MA. He is also professor and chairholder for radio systems at Lund University, Sweden. Dr. Molisch has done research in the areas of SAW filters, radiative transfer in atomic vapors, atomic line filters, smart antennas, and wideband systems. His current research interests are MIMO systems, measurement and modeling of mobile radio channels, and UWB. Dr. Molisch has authored, co-authored or edited four books (among them the recent textbook, *Wireless Communications*, Wiley-IEEE Press), eleven book chapters, some 90 journal papers, and numerous conference contributions. Dr. Molisch is an editor of the *IEEE Transaction on Wireless Communications*, co-editor of recent special issues on MIMO and smart antennas (in the *Journal on Wireless Communications and Mobile Computing*), and UWB (in *IEEE Journal on Selected Areas in Communications*). He has been member of numerous TPCs, vice chair of the TPC of VTC 2005 spring, and general chair of ICUWB 2006. He has participated in the European research initiatives "COST 231," "COST 259," and "COST273," where he was chairman of the MIMO channel working group, he was chairman of the IEEE 802.15.4a channel model standardization group, and is also chairman of Commission C (signals and systems) of URSI (International Union of Radio Scientists). Dr. Molisch is a Fellow of the IEEE and recipient of several awards.